Correlating the Viscosity and Rate of Water Diffusion in Semi-Solid Gel-Forming Aerosol Particles

Craig S. Sheldon[1], Jorge Salazar[1], Teresa Palacios-Diaz[2], Katie Morton[2], Ryan D Davis[3,4], and James F Davies[1]*

1. Department of Chemistry, University of California Riverside, Riverside CA 92521

2. Trinity University, Department of Chemistry, San Antonio, TX 78212

3. Sandia National Laboratories, Materials Reliability Department, Albuquerque NM 87123

4. University of New Mexico, Department of Chemistry and Chemical Biology, Albuquerque, NM 87131

** Corresponding author: jfdavies@ucr.edu*

Abstract

Aerosol particles are known to exist in highly viscous amorphous states at low relative humidity and temperature. The slow diffusion of molecules in viscous particles impacts the uptake and loss of volatile and semi-volatile species and the rate of heterogenous chemistry. Recent work has demonstrated that in particles containing organic molecules and salts, the formation of a two-phase gel states is possible, leading to observations of rigid particles that resist coalescence. The way that molecules diffuse and transport in gel systems is not well characterized. In this work, we use an electrodynamic balance to levitate sample particles containing a range of organic compounds in mixtures with calcium chloride and measure the rate of water diffusion. Particles of the pure organics have been shown to form viscous amorphous states, while in mixtures with divalent salts, coalescence measurements have revealed the apparent solidification of particles, consistent with the formation of a gel state facilitated by ion-molecule interactions. We report in several cases that water transport can actually be increased in the rigid gel state relative to the pure compound that forms a viscous state under similar conditions. These measurements reveal the limitations of using viscosity as a metric for predicting molecular diffusion, and that the gel structure that forms is a much stronger controlling factor in the rate of diffusion. This underscores the need for diffusion measurements as well as a deeper understanding of non-covalent molecular assembly that leads to supramolecular structures in aerosol particles.

TOC Figure

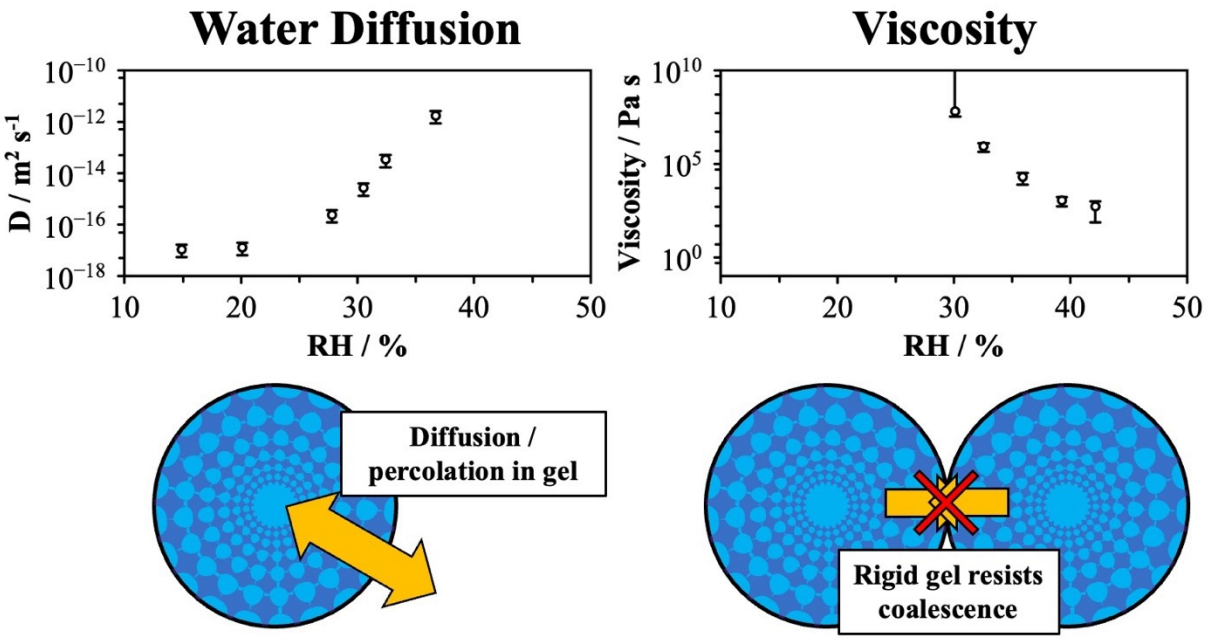

Keywords: water diffusion, particle phase, viscosity, gel formation, ion-molecule interactions, organic-inorganic mixtures

1. Introduction

Aerosols in the atmosphere serve an important role in regulating climate through reflecting and refracting solar radiation and serving as cloud nucleation sites.[1,2] In urban environments, aerosols contribute to the reduction of air quality, with significant negative impacts on health and visibility, and serve as vectors for disease transmission.[3–5] In engineering application aerosols are used to produce dry powders by spray drying and for the dispersal of chemical constituents in agriculture, household products and cosmetics.[6,7] Underpinning the role and impact of aerosol in these fields are the physical and chemical properties of the constituent aerosol particles, such as their hygroscopicity, viscosity, diffusion, and phase morphology, all of which depend upon the composition of the aerosol.[8,9] Additionally, if a particle contains hygroscopic compounds, such as salts and oxygenated organic molecules, the environmental relative humidity (RH) will control the extent of water equilibrium, which in turn controls the phase state of the particle and its rheological properties.[10–13]

In particles containing mixtures of organic compounds and salts, the hygroscopic behavior is typically assumed to be driven by the salt, and the resulting behavior follows a contribution-weighted average of the components. For example, when a salt is added to an organic particle, it is usually expected that the viscosity of the resulting mixtures will decrease due to the addition of hydrophilic ions that increase the water content of the particle. However, recent work has clearly demonstrated that this is not always the case and it has been shown that when atmospherically-relevant amounts of ammonium sulfate (AS), a common inorganic component of the atmosphere, is added to citric acid particles, the hygroscopicity decreases while the viscosity significantly increases.[14] Interestingly, the rate of water diffusion, inversely related to the viscosity according to the Stokes-Einstein relationship, was found to increasingly decorrelate from the viscosity as more AS was added. In mixtures of AS and sucrose, the viscosity has been shown to decrease when AS is added, as would be expected given the increased hygroscopic growth.[15] Dications (Ca^{2+}, Mg^{2+} etc. that are common in sea water[16]) have been shown to induce the formation of a gel state in particles containing oxygenated organic molecules, leading to sharp increases in the viscosity of the system.[17,18] It should be noted that these effects have not been observed with NaCl. In general, there are two characteristic responses on the addition of inorganic components: (1) a

decrease in viscosity due to additional water uptake, where the water acts as a plasticizer; or (2) an increase in apparent viscosity due to interactions between organic molecules and the ions in solution. In the latter case, these ion-molecule interactions can lead to long-range supramolecular assembly and the formation of a gel structure. The nature of the organic functional groups and the specific ions will determine which of these responses will dominate the behavior. Gel states have also previously been observed in particles containing just $MgSO_4$ and water, and diffusion measurements show a sharp decrease in the rate of diffusion that is effectively modelled using percolation theory.[11,19] In general, the broader connection between viscosity and diffusion in gel states is not well-characterized.

In general, to measure viscosity in bulk liquids, rheometric and flow-based methods are used. However, these bulk measurements cannot measure material properties of aerosol particles due to the strong influence of supersaturation and changes in phase state that occur at low RH. Instead, aerosol-based methods for characterizing viscosity have been developed that use methods such as coalescence,[17,20] impaction,[21] fluorescence imaging,[22] and flow-based methods.[23,24] Of these, only coalescence measurements allow for the viscosity and phase state of levitated amorphous particles to be probed in the absence of contact with surfaces. Using aerosol optical tweezers and electrodynamic balance (EDB) methods for particle levitation, coalescence can be performed in controlled environmental conditions, allowing for a rigorous exploration of the phase and rheology of particles.

While viscosity is relatively easy to measure in aerosol, the physical quantity of interest for predicting the chemical lifetime of a particle is the rate of molecular diffusion. Diffusion, which is typically inversely related to viscosity, regulates the rate of which molecules move within the particle along a chemical activity gradient. This impacts the uptake and loss of volatile and semi-volatile chemical species, the rate of penetration by gas phase oxidants, and the rate of chemical evolution.[25–28] There are several ways to measure diffusion in aerosol particles, though efforts have broadly been limited to the diffusion of water.[11,29–31] Measuring the diffusion rate of other molecules in a viscous medium is challenging, and has been achieved only in a few cases, such as for isotopically labeled sucrose or for semi-volatile species evaporating from viscous [32,33]. Measuring the diffusion rate of water is more common, but still presents significant challenges due

to the fact that the diffusion coefficient is heavily dependent on the amount of water in the particle. Therefore, any method that disturbs the amount of water in the aerosol must account for this. In our previous work we demonstrated a method to measure the diffusion coefficient with minimal RH perturbation, yielding results that agreed well with other methods, such as isotope exchange, that do not impose a change in the total amount of water.[14]

To connect viscosity and diffusion, a first approximation is the Stokes-Einstein (SE) relation, which assumes a large sphere diffusing through a viscous continuum. This approximation is known to breakdown when a small molecule, such as water, is diffusing through a viscous matrix consisting of finite sized molecules. A modification to SE, known as the fractional Stokes-Einstein (fSE), includes an exponent as a scaling factor that has been shown to scale with the ratio of the size of the diffusing molecule to the size of the molecules in the viscous matrix[34,35].

Although gel states have been shown to slow transport that is interpreted with a reduced effective diffusion coefficient, the unique phase state of a gel leads to much more complex behavior involving both diffusion and percolation.[11,19,36] Furthermore, the ability to measure a true viscosity in a two-phase system is limited and gels can exhibit non-Newtonian behavior whereby they cannot be fully described with a single dynamic viscosity. Nevertheless, effective diffusion coefficients and apparent viscosity are relatively easily measured quantities, even for particles that form gel states, and reveal important information on how a system will behave as a function of RH. However, for a two-phase system, simple viscosity measurements using, e.g., particle coalescence, might not fully reflect the underlying molecular details. For example, a highly-viscous, rigid aerosol particle that does not coalesce might still have liquid pores through which species can readily diffuse[14,17]. To understand diffusion in gel states, it is necessary to expand beyond aerosol viscosity measurements. The application of SE or fSE to the properties of gels has not been explored and we lack a rigorous exploration of how viscosity and diffusion are related in these systems.

In this work, we report measurements of the effective diffusion coefficients of water in particles that are known to form gel states under certain environmental conditions. We first explore magnesium sulfate as a single component gel forming system, and then explore mixtures of

oxygenated organic molecules with $CaCl_2$. Previous work has reported the apparent viscosity of pure glucose (Glu), sorbitol (Sor), gluconic acid (GluA), and glucuronic acid (GlucA) as a function of relative humidity (RH), in addition to the corresponding mixtures with $CaCl_2$. Richards et al.[17,37] revealed that the addition of $CaCl_2$ led to the formation of rigid gel particles that resisted coalescence at mid-ranged RH's. In this work, we measure the hygroscopicity and effective diffusion coefficients of water in particles containing oxygenated organic molecules and $CaCl_2$. A linear quadrupole electrodynamic balance (LQ-EDB) was used to levitated sample particles and Mie resonance spectroscopy (MRS) was used to characterize size and response to changes in environmental conditions. From existing data characterizing the apparent viscosity of these samples, we explore the correlation between the phase state and viscosity and the rate of diffusion.

2. Materials and Methods

2.1 Sample Preparation and Safety

The chemicals used in this study were purchased and utilized without additional purification. Sample particles containing pure $MgSO_4$ (Fisher Chemical 99%), and glucose (Glu, Sigma-Aldrich >99.5%), sorbitol (Sor, Sigma-Aldrich >98%), gluconic acid (GluA, Merck 50% w/w water), and glucuronic acid (GlucA, Sigma-Aldrich >98%), along with their mixtures with $CaCl_2$ (Sigma-Aldrich >93%), were prepared from aqueous solutions. Lithium chloride particles, used as a probe to measure RH within the chamber, were trapped simultaneously with the sample particles in accordance with our previously described dual-droplet method. Particles were generated following solvent evaporation from droplets produced using a microdroplet dispenser (Microfab MJ-ABP-01), as described in our previous work and described briefly here. Dilute aqueous solutions with a total solute concentration of 4 to 6 g/L were prepared and transferred to the microdroplet dispenser. Solutions of pure components and equimolar mixtures of organic samples with $CaCl_2$ were prepared. Individual droplets with diameters on the order of 50 μm were generated by application of a voltage pulse to the dispenser and excess solvent evaporated to yield particles with a radius of 3 to 8 μm. A charge was induced on the droplets during their formation leading to a net charge on the particle, allowing them to be levitated using the electric fields of the LQ-EDB.[38,39].

For all measurements, safety procedures were followed according to established best practices. No unexpected or unusually high safety hazards were encountered.

2.2 Particle Levitation

A linear quadrupole electrodynamic balance (LQ-EDB) was used to levitated multiple particles for extended periods of time using electric fields. Sample droplets produced from the microdroplet dispenser were given a net charge on the order of 10 to 100 fC by inductive charge separation due to the presence of an electrode operated at a voltage of 200 to 500 V. Droplets travel horizontally into the trapping chamber and become confined in the central axis of the linear quadrupole due to the electric fields. A 532 nm laser with an operating power of < 5 mW was used to visually verify introduction and trapping of droplets. Droplets fall vertically along the axis of the linear quadrupole due to a gravitational force and drag force from an air flow, at 200 sccm, and reach a stable trapping position when the vertically acting forces are balanced by a repulsive electrostatic force generated by an applied DC voltage (10 to 300 V) applied to a disk electrode. A CMOS camera was used to image particles in the trap to verify and stabilize the vertical position using a PID feedback loop, programmed using LabVIEW software, to control the DC voltage applied to the balancing electrode.

The RH in the chamber was controlled by introducing a mixture of dry and humidified nitrogen. The RH was monitored using the dual-droplet method with LiCl as a probe particle.[40] The probe acts as an accurate *in-situ* measurement of the RH in the chamber and reveals both the magnitude of the RH and the time dependence of any changes. To achieve the dual-droplet configuration, two dispensers and two induction electrodes were used to introduce the sample and probe droplets into the LQ-EDB simultaneously. The probe and sample particles were periodically moved up and down in the trap to measure the broadband scattering spectra of both particles in a consecutive manner.

2.3 Broadband Spectroscopy

A red LED was used to illuminate a single particle and the backscattered spectrum was collected by optical fibers and delivered to a spectrometer (Ocean Insight HR4000). Spectra were collected with 1 s of exposure time, with both the probe and sample droplet switching every 10 s to collect both simultaneously. Photons of light with specific wavelengths, according to the size and refractive index of the droplet, form standing waves within the droplet and propagate around the circumference to form whispering gallery modes (WGM's). The backscattered spectrum contains

sharp peaks that correspond to WGM's that are analyzed offline to determine the wavelength positions. These are compared with Mie theory predictions using the algorithms developed by Preston and Reid and allow the size and RI to be determined.[41,42] To validate the output, the full spectrum is compared to a simulated spectra using Mie theory and agreement is verified by-eye.

2.4 Water Diffusion Measurements

The full procedure to characterize water diffusion was discussed in our earlier work.[14] Briefly, a sample particle was brought to the measurement RH and allowed to equilibrate. Once equilibrated, the RH was raised or lowered in a 1% step, initiating either water uptake or loss, and the particle responded accordingly via a change in size. The response of a particle was characterized using the time-dependence of the wavelength of peaks in the Mie resonance spectra. A half-life (τ) was determined by fitting a stretched-exponential function to the response (s) using Equation 1:[43]

$$s(t) = (s_o - s_\infty)e^{\left(-\frac{t}{\tau}\right)^\beta} + s_\infty \qquad (1)$$

The numerical values of τ and β from either Equation 1 were used to solve for half-life of the response:

$$t_{1/2} = \left|\tau ln\,(0.5)^\beta\right| \qquad (2)$$

The half-life is related to the diffusion rate of water in the particle according to:

$$D = \frac{a^2 ln\,(2)}{\pi^2 t_{1/2}} \qquad (3)$$

where a is the radius of the particle and $t_{1/2}$ is the half time from Equation 3. It should be noted that this procedure assumes that the response to a step-change in RH has a single timescale. In a gel, which is a two-phase system, it might be reasonable to assume multiple timescales as the fluid and solid portions of the gel respond on fast and slow timescales, respectively. Our data do not clearly show multiple timescales and throughout this manuscript we report effective diffusion coefficients that assume a single timescale controls the response.

2.5 Hygroscopic Growth Measurements:

To measure the hygroscopic growth of the samples, a probe and sample droplet were trapped, and the dry size was found by holding the sample at 0% RH. The RH was then raised to the

measurement RH, and the droplet was allowed to equilibrate. The size was recorded at 5% RH intervals over the relevant RH range for each system. Measurements were performed on both pure organic particles and mixtures of organic with $CaCl_2$. The calculated radial growth factor (rGF) was then compared to the AIOMFAC model, which predicts particle behavior based on the composition and functional groups of the chemicals that make up the particle.[44,45] A simple volume-additive approach was used to estimate the density of the particle to convert the model output to a comparable metric to the experiments.

3. Results

3.1 Water Transport in Binary Gel Particles

To verify the methodology is consistent with previous work on water diffusion in gels, we explored water transport in $MgSO_4$ particles as a function of RH. Sample particles were exposed to a 1% step increase and decrease in RH and the response was determined based on the change in the wavelength of individual peaks in the Mie resonance spectrum. An example of the time dependence for a 1% step in RH for $MgSO_4$ is shown in Figure 1A and Figure 1B, revealing very different timescales depending on the RH. A stretched exponential function was fit to the data and the half-life time was determined, assuming the process occurs with a single timescale, as discussed in Section 2.4. The effective diffusion coefficient of water estimated from these data are shown in Figure 1C as a function of RH, along with previous measurements from Davies and Wilson[11] and Price et al.[39]. Although there is some discrepancy in the RH at the gel transition, identified by the sharp decrease in D_w as the RH decreases, the current work shows behavior consistent with rapid onset of a gel structure leading to slowed water transport. These data are consistent with percolation theory, which describe how material can move in a porous systems based on the pore size, packing efficiency, and porosity of the material.[28,46]

Measurements of the apparent viscosity of $MgSO_4$ gel particles were performed using the coalescence approach detailed by Richards et al.[37] Here, the range of viscosity values measured was extended to higher RH than was possible in Richards et al. by incorporating a high-speed camera. These data also show behavior that is characteristic of a phase transition, with the viscosity showing a clear change in its trend versus RH at a point consistent with the onset of gel formation. These data are shown in Figure 1D.

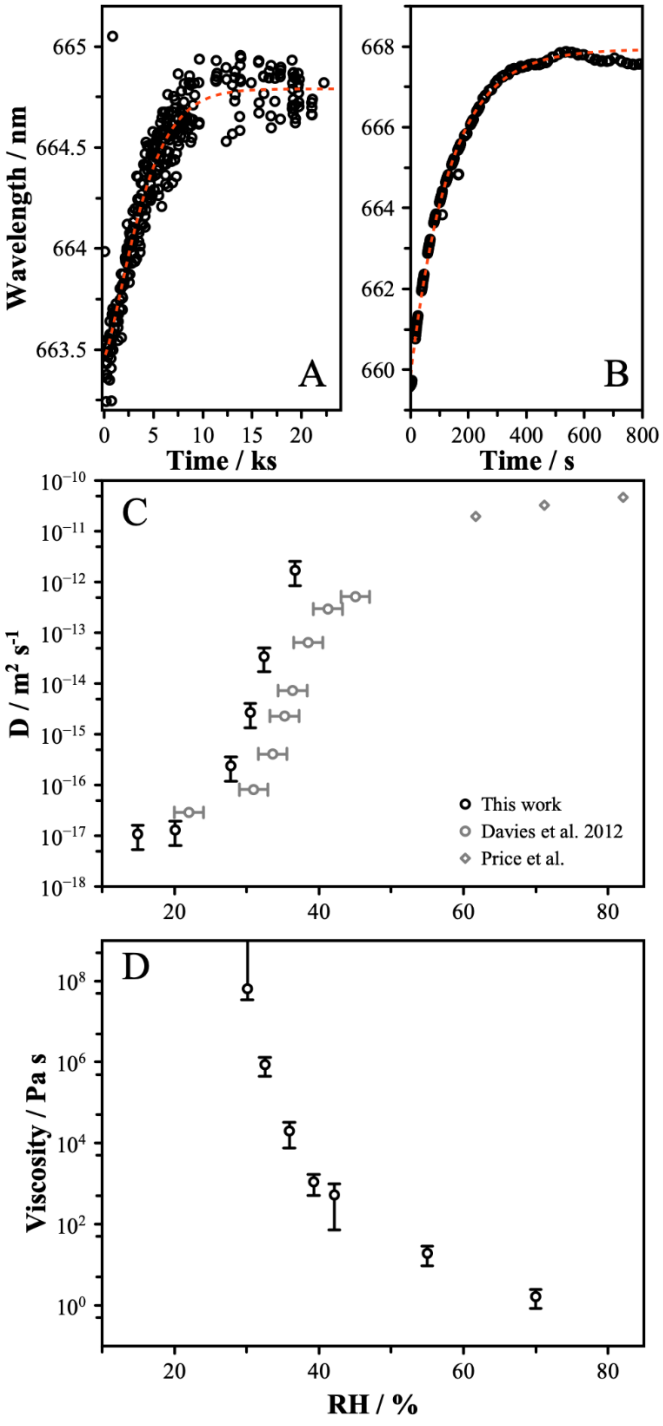

Figure 1: Characteristic response of $MgSO_4$ particles at A) 15% RH; and B) 35% RH. C) Diffusion coefficients determined using Equation 3 showing the sudden onset of slowed diffusion, consistent with previous data. D) The viscosity of $MgSO_4$ shows a sharp upward inflexion as the RH decreases through the gel transition RH. Note that data at 70% represents a single trial using a new high-speed camera applied to the experimental platform reported by Richards et al.

3.2 Water Transport in Binary Viscous Particles

Previous work has demonstrated the formation of viscous amorphous states at low RH for pure organic particles containing oxygenated species. In particles containing sucrose, citric acid, and a range of other organic species, high viscosity is associated with reduced rates of water diffusion.[14,17,20] The viscosity data of Richards et al.[37] for pure gluconic acid, glucose, sorbitol and glucuronic acid are reproduced in Figure S2, revealing that these samples also experience a clear increase in viscosity as the RH decreases. In this work, we characterized the diffusion coefficient of water in these samples, and the data are shown as a function of RH in Figure 2A-D (solid symbols). In all cases, a slowing of water transport was observed to correlate with decreasing RH with an approximately linear decrease in the logarithm of the diffusion coefficient with RH. This dependence is typical of a transition to a viscous state and the sharp decrease in diffusivity associated with gel formation is not observed. These data support the assertion that binary particles containing only organic molecules and water will form viscous amorphous states at low RH. Across these samples, glucose particles are observed to yield the slowest rate of diffusion, with D = 10^{-15} m^2 s^{-1} at 20% RH, while sorbitol particles only reach around 4×10^{-14} m^2 s^{-1} at the same RH.

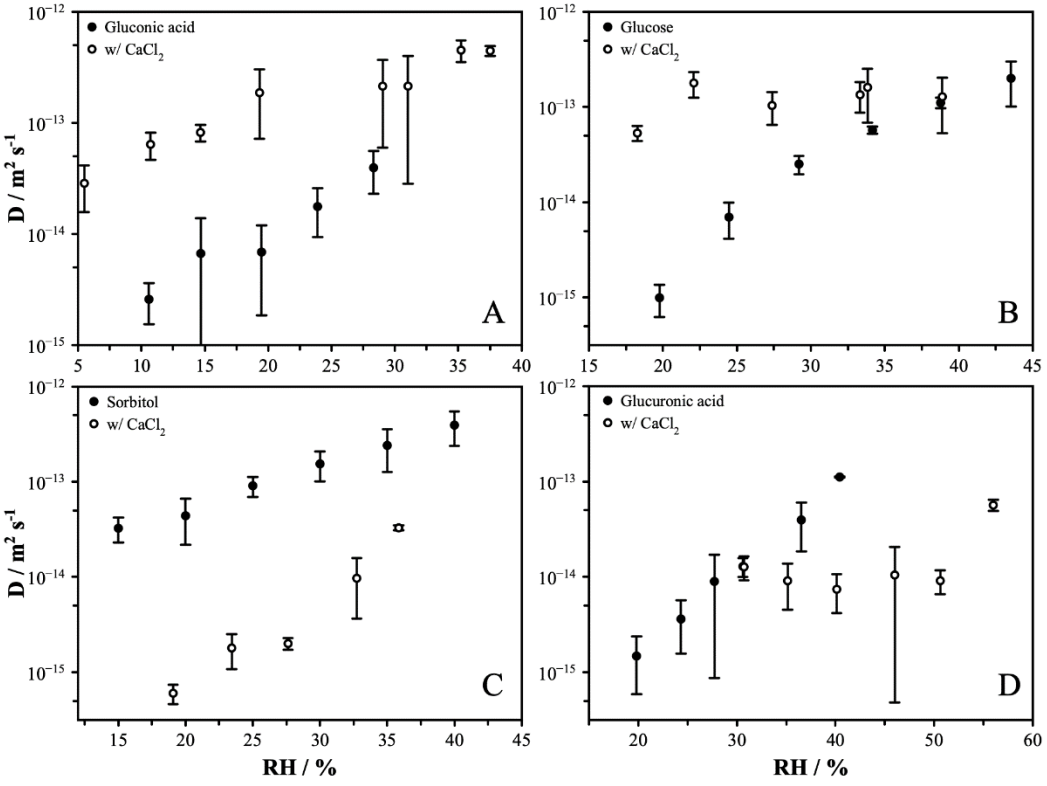

Figure 2: Diffusion coefficients for binary (solid circles) and ternary (open circles, with $CaCl_2$) systems of A) gluconic acid; B) glucose; C) sorbitol; and D) glucuronic acid.

The monotonic decrease in the rate of water diffusion coincides with a decrease in the size of the response of the particles to the 1% step in RH, shown in Figure S3A as the magnitude of the change in the wavelength. These data further demonstrate that no phase transition is occurring and the change in the viscosity and diffusion rates can be attributed to a steady decrease in the amount of water present as a function of RH (reported in Section 3.4).

3.3 Water Transport in Ternary Particles Containing $CaCl_2$

Following the addition of $CaCl_2$ in equimolar quantities to these organic particles, the apparent viscosity has been shown to increase significantly. Previous work using coalescence to measure the viscosity of ternary particles of the samples was performed by Richards et al.,[37] and we summarize the results in Figure S2. At low RH, particles were observed to reach states in which coalescence is not observed over measurement timescales. These observations are attributed to the formation of a gel state that forms as a result of strong ion-molecule interactions between the oxygenated function groups of the organic molecules and the divalent Ca^{2+} ions in the mixture.

In this work, we characterize the rate of water diffusion in these samples. The addition of $CaCl_2$ to the organic systems results in observed behavior that is highly system specific. In general, the 1% step changes in RH yielded larger magnitudes of change in the peak positions at high RH compared to the pure particles, and lower changes in the magnitude of the change at low RH, following the formation of a gel state. These data are shown in Figure S3B. The same fitting procedure was applied to the response and the analysis was carried out as described earlier. In Figure 3A-D, we show the resulting effective diffusion coefficients as a function of RH measured for equimolar mixtures of $CaCl_2$ with each organic. In the case of sorbitol, a clear slowing of water transport is observed relative to the pure organic component, consistent with our previous work using a different method.[37] The diffusion coefficients decrease by up to two orders of magnitude at low RH compared to pure sorbitol, although the trend does not exhibit the marked step-change within the RH range that was characteristic of $MgSO_4$ gel particles. In gluconic acid particles, the addition of $CaCl_2$ leads to an increase in the measured rates of water diffusion, with diffusion occurring

between 10 and 50× more rapidly than in the pure component case within the RH range studied. For glucuronic acid and glucose, the addition of $CaCl_2$ has a less clear effect on diffusion. Ternary glucose particles show diffusivity that varies minimally with RH and remain at the upper end of the resolvable range for D, and above the measured rate of diffusion in the binary system. Ternary glucuronic acid particles show the most variable behavior, with an initial decrease in D, below that of the binary system, as the gel range is entered, with a subsequent plateau.

Examination of the magnitude of the wavelength response as a function of RH, shown in Figure S3B, reveals some interesting observations when comparing against the binary data in Figure S3A. The ternary systems (except glucose) show a step change in the magnitude of the response – for sorbitol this occurs at 25 to 30% RH and glucuronic acid at 50 to 55% RH, both consistent with the RH at gel formation indicated by viscosity. For gluconic acid, the response shows this decrease at 25 to 30% RH, which is lower than indicated by viscosity measurements (around 50%). The viscosity data indicate gel formation in glucose at around 25%, while the wavelength change magnitude indicate we do not observe gel formation for this system in these measurements or the gel state does not behave in a way that is consistent with other aerosol gel states that have been studied.

3.4 Hygroscopicity of Binary and Ternary Particles

To characterize how the composition of the particles are influenced by the addition of $CaCl_2$, we characterized the hygroscopic growth of each sample using a dual-droplet approach. Briefly, sample particles were levitated alongside an RH probe particle (LiCl) and the change in size of the sample was correlated with the change in RH determined from the probe. Particles were left at each RH for sufficient timescales to achieve equilibrium, as established from the diffusion measurements. The pure organic particles show limited hygroscopic growth, as seen in Figure 3, in agreement with the predictions from the AIOMFAC model.[44,45] The AIOMFAC model calculates the activity coefficients of each component in a mixture of known composition. The contributions to the excess Gibbs energy from short-range, mid-range, and long-range interactions are determined and the partial derivative of the Gibbs energy with respect to the concentration of each component is found. The model output reports the composition in terms of mass and mole fractions, and the activity of each component. To convert the mass fraction of the AIOMFAC

model to a radial growth factor, we calculate the volume contribution of each component in the mixture using the respective pure component densities. Then, the sum of the volumes is used to calculate the spherical-equivalent radius and the growth factor is estimated. Although there are some discrepancies, for example the hygroscopic growth of glucuronic acid is slightly over-estimated, the generally good agreement is validation that the model accurately accounts for the behavior of individual species. We further measured the hygroscopicity of $CaCl_2$ (Figure S4), which exhibits efflorescence and deliquescence behavior that makes measurements of the absolute radial growth factor challenging. In comparison to the AIOMFAC model, if we assume a measurement dry size to yield a radial growth factor in agreement with the AIOMFAC model at an arbitrary RH (40% was used here), then good agreement across the full range of measured values is observed.

Having established that binary systems of the components of interest are well-characterized by AIOMFAC, we go on to compare the results for the ternary mixtures. These are shown in Figure 3. From the measurements, the change in hygroscopicity on addition of $CaCl_2$ is low, with gluconic acid showing the largest increase in hygroscopicity while the other compounds show a decrease (glucose) or a small increase (sorbitol and glucuronic acid). The AIOMFAC predictions show significant over-estimation of the hygroscopic growth in all cases, with the predicted behavior showing much more bias towards the hygroscopic growth of $CaCl_2$ than is observed experimentally. This discrepancy may be associated with the strong interactions of Ca^{2+} with the oxygen functional groups present in the organic molecules, leading to less favorable interactions with water.

Although the discrepancy between the predicted rGF and measured likely arises from an inaccurate representation of the interactions between ions and molecules in the AIOMFAC model for these systems, another source of error that may contribute arises from how the density is used to convert the model output to a radial growth trend that is comparable with the measurements. Here, we assume density is ideally additive, and we use the density of the pure component. However, $CaCl_2$ is a strong electrolyte, and the solvation of Ca^{2+} may lead to an increase in the density of the solution relative to the simple assumption. This would lead to modelled data overestimated the radial GF. The partial molar volume of $CaCl_2$ in dilute solutions is known to be less than the

estimated molar volume of the solid,[47] but these data are far from the concentrations encountered in this work. It is unlikely that the range of possible values of the real partial molar volume would change the overall radial growth factor trend to any significant degree.

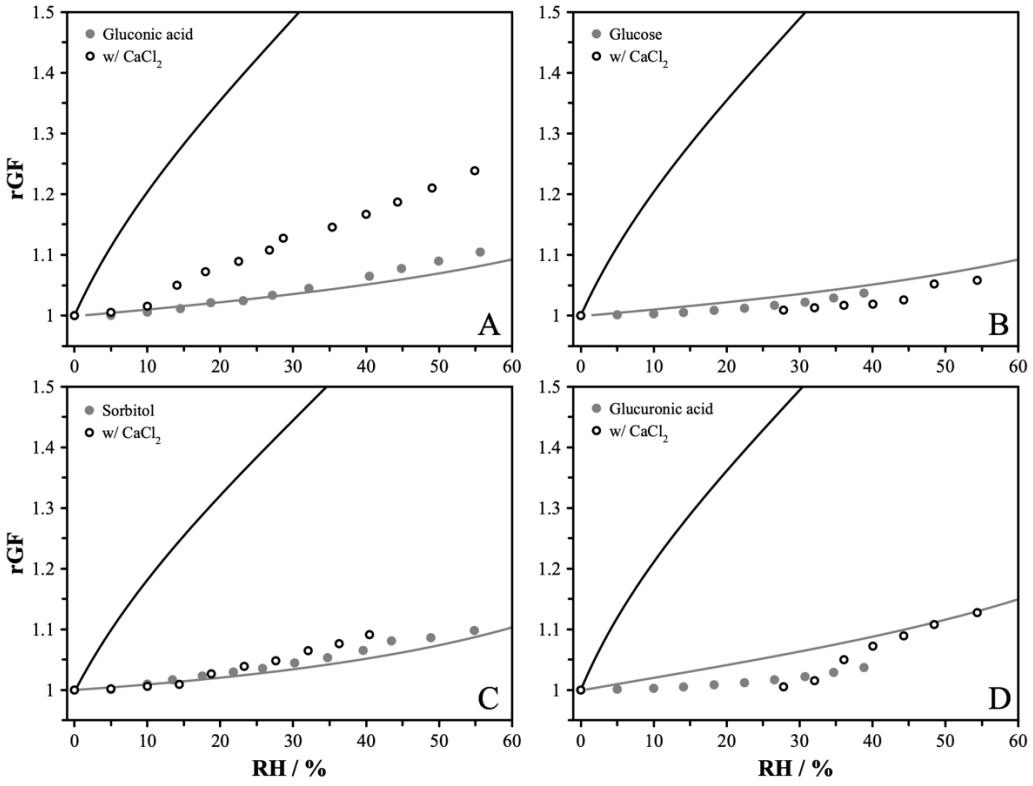

Figure 3: Hygroscopic growth measurements for binary (solid circles) and ternary (open circles, with $CaCl_2$) systems of A) gluconic acid; B) glucose; C) sorbitol; and D) glucuronic acid. The gray solid line indicates the AIOMAC prediction for the binary system while the black solid line indicates the AIOMFAC prediction for the ternary system.

4. Discussion

4.1 Correlating Diffusion and Viscosity in Binary Viscous Particles

The Stokes-Einstein relationship describes the connection between viscosity and diffusion under the assumption of a large diffusing sphere, with radius r, in a continuous medium of viscosity μ, according to:

$$D = \frac{k_B T}{6\pi\eta r}$$

While this relationship effectively describes the inverse-correlation between viscosity and diffusion, it has been shown inaccurate, by several orders of magnitude, when accounting for the

diffusion of small molecules such as water. Small molecules exhibit diffusion rates that are much faster than expected based on this equation. As an empirical correction to the Stokes-Einstein relationship, the fractional Stokes-Einstein relationship introduces an exponent to yield the equation:[34]

$$\frac{D}{D_0} = \left(\frac{\eta_0}{\eta}\right)^{\xi}$$

where D_0 and μ_0 are the diffusion coefficient and viscosity at a known point, here taken to be that of pure water and ascribed the values 10^{-9} m^2 s^{-1} and 0.001 Pa s, respectively. The value of the exponent, ξ, was parameterized against the ratio of the size of the diffusing molecule (here, H_2O) and the average size of molecules in the viscous matrix, $R_{\mathrm{diff}}/R_{\mathrm{matrix}}$.

To compare the measurements of viscosity and diffusion that span different RH points, we apply an empirical parameterization to obtain a function that describes how the two RH-dependent variables vary with each other. Using these derived relationships, we plot the diffusion coefficient of water as a function of the viscosity in Figure 4 for all the binary systems explored in this work. We further show in the plot fraction Stokes-Einstein contours as a comparison. For the organic systems, the rate of diffusion is higher than expected based on SE, and indeed the data follows the fSE prediction with exponents that range from around 0.6 to 0.8 over the measured span of both datasets. Based on the estimated molecular radii derived from the density and molecular mass (Table 1), the corresponding $R_{\mathrm{diff}}/R_{\mathrm{matrix}}$ is around 0.55 for all of these compounds. These data fall within the 95% confidence interval reported by Evoy et al.[34] for the parameterization of ξ versus $R_{\mathrm{diff}}/R_{\mathrm{matrix}}$.

Table 1: Molecular weight, density, molar volume, molecular radius, radius ratio of water (0.2 nm) with respect to each component, and the gel forming RH according to coalescence measurements. *Gel formation RH as indicated by this work, where different from Richards et al.

	M_W	ρ / g cm^{-3}	V_M / cm^3 mol^{-1}	R / nm	$R_{\mathrm{diff}}/R_{\mathrm{matrix}}$	Gel RH / %
Sorbitol	182	1.49	122	0.36	0.55	25
Gluconic acid	196	1.46	134	0.38	0.53	48, 25*
Glucuronic acid	194	1.7	114	0.36	0.56	48
Glucose	180	1.56	115	0.36	0.56	25, N/A*
$MgSO_4$	120	2.66	45	0.26	0.76	30

$CaCl_2$	111	2.15	52	0.27	0.73	N/A

For the gel-forming $MgSO_4$, the rate of diffusion is much faster than expected based on SE, and the fSE exponent ranges from around 0.4 to 0.5. From the density and molecular mass, $R_{\mathrm{diff}}/R_{\mathrm{matrix}}$ for $MgSO_4$ is ~0.76 nm. Based on the parameterization of Evoy el al., these data fall outside the 95% confidence interval and such a ratio would be expected to show ξ values around 0.8. Given that the parameterization here was developed only with viscous systems and not gels, it is not surprising that the result for $MgSO_4$ is physically unreasonable. In the case of the gel, the rate of water transport is limited by diffusion and by the structure of the gel, with fluid constrained to travel through pores and channels of a finite size. In previous work, percolation theory was used to describe the change of diffusion coefficient as a function of RH.[11] With the assumption that the diffusion coefficient of water in the fluid phase was the same as in a saturated aqueous solution, the effectiveness of this model showed that water transport was only limited by the gel structure and was not connected to the apparent viscosity of the system. This is broadly consistent with known theories on diffusive transport in gels that connect the diffusion coefficient to a function of the size of the diffusing molecule and the correlation length of the gel, a parameter that describes the gel structure in cross-linked polymer systems.[48] Thus, although fSE is a useful framework to apply to explore diffusive behavior in viscous systems, it does not appear capable of producing meaningful insights into the behavior of gels. In the case where the fluid is viscous, transport within a gel structure becomes more complicated. We explore this concept further for the case of ternary systems.

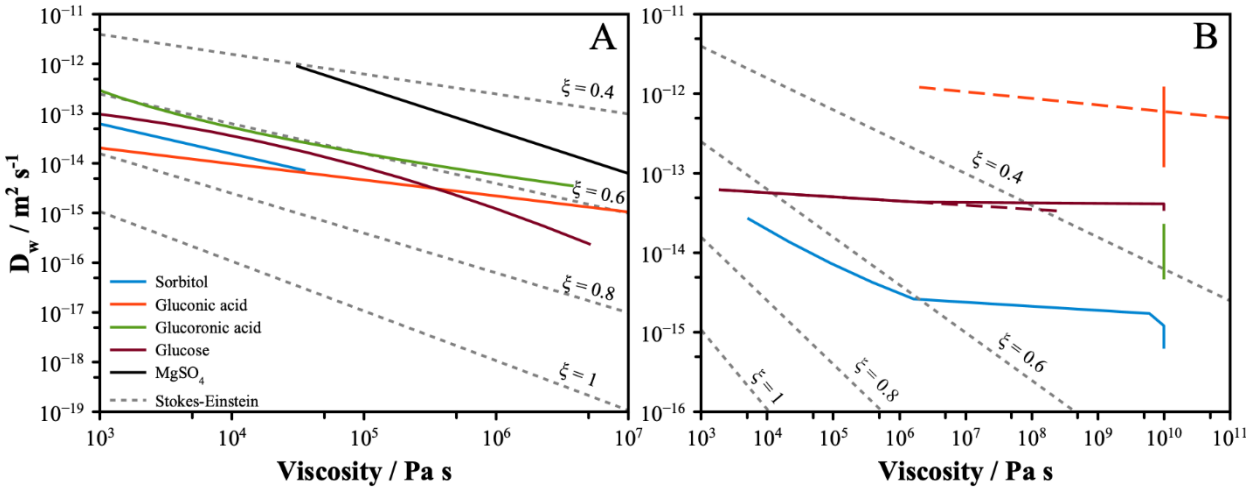

Figure 4: Stokes-Einstein plots of diffusion versus viscosity for: A) binary; and B) ternary systems. Solid lines represent parameterized experimental measurements using data from this work and Richards et al., while the dashed lines represent an extrapolation of the pre-gel viscosity data of Richards et al. to the gel forming point identified in this work. Gray dotted lines show fractional Stokes-Einstein predictions with varying values of the exponent ξ.

4.2 Correlating Diffusion and Viscosity in Ternary Mixtures

The apparent viscosity was used to characterize the onset of the gel transition by the rapid increase in the viscosity by several orders of magnitude for a small decrease in RH. These onset RH values are shown in Table 1. For glucuronic acid and gluconic acid, the gel state was present for all measurements of water diffusion, and no diffusion limitations were measured above the gel forming RH, indicating sufficient water present to fully plasticize the particles. Following formation of the gel, gluconic acid particles show a monotonic decrease in the rate of water diffusion while the viscosity data indicate the particle is fully rigid. In glucuronic acid, the rate of water diffusion appears to plateau and a limited dependence on RH is not observed outside of experimental error. A similar plateau was observed in glucose particles above the gel transition, and no notable change in diffusion was observed following gel formation. However, it may be the case that the glucose does not form gel in the measurements reported here, evidenced by a lack of clear change in the wavelength response magnitude, as discussed earlier. Finally, sorbitol shows a monotonic decrease in diffusivity with decreasing RH but with no notable change in the trend when the gel transition is reached. A Stokes-Einstein plot for the gel states is shown in Figure 4B. The samples that were in gel states across all diffusion measurements are ascribed a constant viscosity of 10^{10} Pa s.

In ternary mixtures of components that form gel states, it is clear that effective diffusion and apparent viscosity become drastically disconnected. When compared to the fS-E relation, the relationship between these parameters is not accurately represented and, in conditions where the particles are rigid, the unchanging apparent viscosity is fully decorrelated with diffusion. This breakdown comes from the more complex nature of mass transport in two-phase gel particles, where a stiff network can exist that prevents particle coalescence, but mass transport may still occur readily through liquid contained within the pores of the rigid gel structure. Prior to a gel transition, the strong interactions between organic molecules and ions that give rise to elevated viscosity do not appear to strongly reduce the rate of diffusion in a consistent manner. Only in particles containing sorbitol and $CaCl_2$ is true viscous behavior observed prior to the gel state. After gel formation, the concept of viscosity breaks down and the applicability of correlating diffusion with apparent viscosity becomes limited.

Based on how the hygroscopicity varies in these systems on additional of $CaCl_2$, the amount of water present is also not a useful indicator of the viscosity and/or diffusion. In gluconic acid, for example, the hygroscopicity is increased relative to the pure organic species on addition of the salt, and the corresponding diffusion coefficients are larger than in the binary case. However, this system also shows the onset of gel formation at high RH, when the water content is still relatively high. This may point towards a gel structure that contains a significant fluid phase in large pores that do not inhibit water diffusion, while the presence of the $CaCl_2$ that remains in solution increases the hygroscopicity of the fluid phase, leading to both more water and faster diffusion. In contrast, ternary sorbitol particles show very little increase in their hygroscopic growth, while the rate of water diffusion is much slower than in the binary particles, even before the onset of the get. This indicates that ion-molecule interactions are important to consider even before any phase transitions occur. In ternary glucose particles, gel formation is expected at a similar RH as in the sorbitol system, however for glucose the rate of diffusion is faster in the ternary system than in the binary system, even though the water content is reduced according to the hygroscopicity data.

Although the amount of water likely plays an important role in the formation of the gel network and influences the rheological properties of the fluid entrained with the gel structure, it is not predictive or indicative of the resulting physical properties of the system. Instead, the rate of

diffusion will be a complex function of the gel structure and the rheological properties of the entrained fluid. Knowledge of the composition of both phases within the gel would be required for a more complete understanding of how the fluid moves within the gel.

Conclusions

In this work we report the diffusion coefficients of water in four binary organic systems and connect the measured values to previously measured viscosity. Although it is widely known that the Stokes-Einstein relationship between diffusion and viscosity breaks down for water diffusion, we demonstrate that the fractional Stokes-Einstein relationship is appropriate in these binary systems in which the particles form viscous states at low RH. We measure the hygroscopic growth of these organics and show agreement to the AIOMFAC model. In ternary systems, where the third component is $CaCl_2$, previous work has established the formation of rigid gel states associated with a significant increase in the apparent viscosity. We report the effective diffusion coefficients of water in these systems and show that correlations with viscosity break down, even when applying the fSE relationship. The hygroscopicity in these systems is suppressed relative to the AIOFAC predictions, but the amount of water does not appear to be strong indicative of the phase state or physical characteristics of the particles.

Our broad interest in understanding the connection between these fundamental physical properties is rooted in the need to correlate easily measurable parameters, such as viscosity, with hard to measure parameters, such as diffusion coefficients, that inform the chemical evolution of aerosol in the atmosphere. Our results indicate that for particles that form traditional viscous states, the fSE approach is effective in allowing diffusion and viscosity to be correlated. However, in organic-inorganic mixtures that exhibit gel transitions, the strong ion-molecular interactions that drive the phase behavior prohibit such a simple relationship from being applicable.

The microscopic structure plays a much larger role in regulating the rate of molecular transport in gel systems, and gel behavior is likely to be an important process due to the prevalence of oxygenated organic species and divalent ions in the atmosphere. This points towards a limitation in the use of viscosity as a metric for predicting molecular transport and a potentially significant underestimate of the rate of molecular transport in many amorphous systems. To explore diffusion

in gel structures further, it will be necessary to better understand the microscopic structure of the particle and the composition of the fluid and solid portions of the gel. Knowledge of both the viscosity and the pore and channel sizes should allow a rigorous analysis of how material transports in a gel structure. Further work is planned using computational methods to provide a molecular-level interpretation of transport in gels. From these data, it will be necessary to develop empirical or semi-empirical relationships that allow the rate of diffusion in gels to be predicted from readily-measured particle parameters. More broadly, this work points to a need to further understand gel states and how they affect the physical properties and transformation processes of aerosol particles. This work provides further evidence that molecular interactions are responsible for significant deviations from expected behavior that cannot be explained through simple mixing rules.

Acknowledgements

J.F.D and C.S.S. acknowledge the support of the NSF through grant CHE-2108004. R.D.D. acknowledges the support of the NSF through grant CHE-2107690. Sandia National Laboratories is a multi-mission laboratory managed and operated by National Technology & Engineering Solutions of Sandia, LLC (NTESS), a wholly owned subsidiary of Honeywell International Inc., for the U.S. Department of Energy's National Nuclear Security Administration (DOE/NNSA) under contract DE-NA0003525. This written work is authored by an employee of NTESS. The employee, not NTESS, owns the right, title and interest in and to the written work and is responsible for its contents. Any subjective views or opinions that might be expressed in the written work do not necessarily represent the views of the U.S. Government. The publisher acknowledges that the U.S. Government retains a non-exclusive, paid-up, irrevocable, world-wide license to publish or reproduce the published form of this written work or allow others to do so, for U.S. Government purposes. The DOE will provide public access to results of federally sponsored research in accordance with the DOE Public Access Plan.

Supporting Information Available

Chemical structures, additional data figures.

References

(1) Lohmann, U.; Feichter, J. Global Indirect Aerosol Effects: A Review. *Atmos. Chem. Phys.* **2005**.
(2) Haywood, J.; Boucher, O. Estimates of the Direct and Indirect Radiative Forcing Due to Tropospheric Aerosols: A Review. *Rev. Geophys.* **2000**, *38* (4), 513–543. https://doi.org/10.1029/1999RG000078.
(3) Kelly, F. J.; Fussell, J. C. Air Pollution and Public Health: Emerging Hazards and Improved Understanding of Risk. *Environ Geochem Health* **2015**, *37* (4), 631–649. https://doi.org/10.1007/s10653-015-9720-1.
(4) Wang, C. C.; Prather, K. A.; Sznitman, J.; Jimenez, J. L.; Lakdawala, S. S.; Tufekci, Z.; Marr, L. C. Airborne Transmission of Respiratory Viruses. *Science* **2021**, *373* (6558), eabd9149. https://doi.org/10.1126/science.abd9149.
(5) Yang, W.; Elankumaran, S.; Marr, L. C. Relationship between Humidity and Influenza A Viability in Droplets and Implications for Influenza's Seasonality. *PLoS ONE* **2012**, *7* (10), e46789. https://doi.org/10.1371/journal.pone.0046789.
(6) Vehring, R.; Foss, W. R.; Lechuga-Ballesteros, D. Particle Formation in Spray Drying. *Journal of Aerosol Science* **2007**, *38* (7), 728–746. https://doi.org/10.1016/j.jaerosci.2007.04.005.
(7) Woodrow, J. E.; Gibson, K. A.; Seiber, J. N. Pesticides and Related Toxicants in the Atmosphere. In *Reviews of Environmental Contamination and Toxicology Volume 247*; de Voogt, P., Ed.; Reviews of Environmental Contamination and Toxicology; Springer International Publishing: Cham, 2019; pp 147–196. https://doi.org/10.1007/398_2018_19.
(8) Bzdek, B. R.; Reid, J. P. Perspective: Aerosol Microphysics: From Molecules to the Chemical Physics of Aerosols. *The Journal of Chemical Physics* **2017**, *147* (22), 220901. https://doi.org/10.1063/1.5002641.
(9) Krieger, U. K.; Marcolli, C.; Reid, J. P. Exploring the Complexity of Aerosol Particle Properties and Processes Using Single Particle Techniques. *Chem. Soc. Rev.* **2012**, *41* (19), 6631–6662. https://doi.org/10.1039/c2cs35082c.
(10) Reid, J. P.; Bertram, A. K.; Topping, D. O.; Laskin, A.; Martin, S. T.; Petters, M. D.; Pope, F. D.; Rovelli, G. The Viscosity of Atmospherically Relevant Organic Particles. *Nat Commun* **2018**, *9* (1), 956. https://doi.org/10.1038/s41467-018-03027-z.
(11) Davies, J. F.; Wilson, K. R. Raman Spectroscopy of Isotopic Water Diffusion in Ultraviscous, Glassy, and Gel States in Aerosol by Use of Optical Tweezers. *Anal. Chem.* **2016**, 6.
(12) Bastelberger, S.; Krieger, U. K.; Luo, B.; Peter, T. Diffusivity Measurements of Volatile Organics in Levitated Viscous Aerosol Particles. *Atmos. Chem. Phys.* **2017**, *17* (13), 8453–8471. https://doi.org/10.5194/acp-17-8453-2017.
(13) Lee, H. D.; Ray, K. K.; Tivanski, A. V. Solid, Semisolid, and Liquid Phase States of Individual Submicrometer Particles Directly Probed Using Atomic Force Microscopy. *Analytical Chemistry* **2017**, acs.analchem.7b02755. https://doi.org/10.1021/acs.analchem.7b02755.
(14) Sheldon, C. S.; Choczynski, J. M.; Morton, K.; Palacios Diaz, T.; Davis, R. D.; Davies, J. F. Exploring the Hygroscopicity, Water Diffusivity, and Viscosity of Organic–Inorganic Aerosols – a Case Study on Internally-Mixed Citric Acid and Ammonium Sulfate Particles. *Environ. Sci.: Atmos.* **2023**, *3* (1), 24–34. https://doi.org/10.1039/D2EA00116K.
(15) Jeong, R.; Lilek, J.; Zuend, A.; Xu, R.; Chan, M. N.; Kim, D.; Moon, H. G.; Song, M. Viscosity and Physical State of Sucrose Mixed with Ammonium Sulfate Droplets. *Atmospheric Chemistry and Physics* **2022**, *22* (13), 8805–8817. https://doi.org/10.5194/acp-22-8805-2022.
(16) Chi, J. W.; Li, W. J.; Zhang, D. Z.; Zhang, J. C.; Lin, Y. T.; Shen, X. J.; Sun, J. Y.; Chen, J. M.; Zhang, X. Y.; Zhang, Y. M.; Wang, W. X. Sea Salt Aerosols as a Reactive Surface for Inorganic and Organic Acidic Gases in the Arctic Troposphere. *Atmospheric Chemistry and Physics* **2015**, *15* (19), 11341–11353. https://doi.org/10.5194/acp-15-11341-2015.
(17) Richards, D. S.; Trobaugh, K. L.; Hajek-Herrera, J.; Davis, R. D. Dual-Balance Electrodynamic Trap as a Microanalytical Tool for Identifying Gel Transitions and Viscous Properties of Levitated Aerosol Particles. *Anal. Chem.* **2020**, *92* (4), 3086–3094. https://doi.org/10.1021/acs.analchem.9b04487.
(18) Song, Y.-C.; Lilek, J.; Lee, J. B.; Chan, M. N.; Wu, Z.; Zuend, A.; Song, M. Viscosity and Phase State of Aerosol Particles Consisting of Sucrose Mixed with Inorganic Salts. *Atmospheric Chemistry and Physics* **2021**, *21* (13), 10215–10228. https://doi.org/10.5194/acp-21-10215-2021.
(19) Cai, C.; Tan, S.-H.; Chen, H.-N.; Ma, J.-B.; Wang, Y.; Reid, J. P.; Zhang, Y. H. Slow Water Transport in MgSO4 Aerosol Droplets at Gel-Forming Relative Humidities. *Phys. Chem. Chem. Phys.* **2015**, *17* (44), 29753--29763. https://doi.org/10.1039/c5cp05181a.

(20) Power, R. M.; Simpson, S. H.; Reid, J. P.; Hudson, A. J. The Transition from Liquid to Solid-like Behaviour in Ultrahigh Viscosity Aerosol Particles. *Chem. Sci.* **2013**, *4* (6), 2597. https://doi.org/10.1039/c3sc50682g.
(21) Virtanen, A.; Joutsensaari, J.; Koop, T.; Kannosto, J.; Yli-Pirilä, P.; Leskinen, J.; Mäkelä, J. M.; Holopainen, J. K.; Pöschl, U.; Kulmala, M.; Worsnop, D. R.; Laaksonen, A. An Amorphous Solid State of Biogenic Secondary Organic Aerosol Particles. *Nature* **2010**, *467* (7317), 824–827. https://doi.org/10.1038/nature09455.
(22) Hosny, N. A.; Fitzgerald, C.; Tong, C.; Kalberer, M.; Kuimova, M. K.; Pope, F. D. Fluorescent Lifetime Imaging of Atmospheric Aerosols: A Direct Probe of Aerosol Viscosity. *Faraday Discuss.* **2013**, *165*, 343. https://doi.org/10.1039/c3fd00041a.
(23) Grayson, J. W.; Song, M.; Sellier, M.; Bertram, A. K. Validation of the Poke-Flow Technique Combined with Simulations of Fluid Flow for Determining Viscosities in Samples with Small Volumes and High Viscosities. *Atmos. Meas. Tech.* **2015**, *8* (6), 2463–2472. https://doi.org/10.5194/amt-8-2463-2015.
(24) Rovelli, G.; Song, Y.-C.; Maclean, A. M.; Topping, D. O.; Bertram, A. K.; Reid, J. P. Comparison of Approaches for Measuring and Predicting the Viscosity of Ternary Component Aerosol Particles. *Analytical Chemistry* **2019**, *91*, 5074–5082. https://doi.org/10.1021/acs.analchem.8b05353.
(25) Wallace, B. J.; Price, C. L.; Davies, J. F.; Preston, T. C. Multicomponent Diffusion in Atmospheric Aerosol Particles. *Environ. Sci.: Atmos.* **2021**, *1* (1), 45–55. https://doi.org/10.1039/D0EA00008F.
(26) Davies, J. F.; Wilson, K. R. Nanoscale Interfacial Gradients Formed by the Reactive Uptake of OH Radicals onto Viscous Aerosol Surfaces. *Chemical Science* **2015**, *6* (12), 7020–7027. https://doi.org/10.1039/c5sc02326b.
(27) Wiegel, A. A.; Liu, M. J.; Hinsberg, W. D.; Wilson, K. R.; Houle, F. A. Diffusive Confinement of Free Radical Intermediates in the OH Radical Oxidation of Semisolid Aerosols. *Phys. Chem. Chem. Phys.* **2017**, *19*, 6814–6830. https://doi.org/10.1039/c7cp00696a.
(28) Shiraiwa, M.; Ammann, M.; Koop, T.; Pöschl, U. Gas Uptake and Chemical Aging of Semisolid Organic Aerosol Particles. *Proceedings of the National Academy of Sciences* **2011**, *108* (27), 11003–11008. https://doi.org/10.1073/pnas.1103045108.
(29) Nadler, K. A.; Kim, P.; Huang, D.-L.; Xiong, W.; Continetti, R. E. Water Diffusion Measurements of Single Charged Aerosols Using H2O/D2O Isotope Exchange and Raman Spectroscopy in an Electrodynamic Balance. *Phys. Chem. Chem. Phys.* **2019**, *21* (27), 15062–15071. https://doi.org/10.1039/C8CP07052K.
(30) Price, H. C.; Mattsson, J.; Zhang, Y.; Bertram, A. K.; Davies, J. F.; Grayson, J. W.; Martin, S. T.; O'Sullivan, D.; Reid, J. P.; Rickards, A. M. J.; Murray, B. J. Water Diffusion in Atmospherically Relevant α-Pinene Secondary Organic Material. *Chemical Science* **2015**, *6* (8), 4876–4883. https://doi.org/10.1039/c5sc00685f.
(31) Lienhard, D. M.; Huisman, A. J.; Bones, D. L.; Te, Y.-F.; Luo, B. P.; Krieger, U. K.; Reid, J. P. Retrieving the Translational Diffusion Coefficient of Water from Experiments on Single Levitated Aerosol Droplets. *Phys. Chem. Chem. Phys.* **2014**, *16* (31), 16677--16683. https://doi.org/10.1039/c4cp01939c.
(32) Marshall, F. H.; Miles, R. E. H.; Song, Y.-C.; Ohm, P. B.; Power, R. M.; Reid, J. P.; Dutcher, C. S. Diffusion and Reactivity in Ultraviscous Aerosol and the Correlation with Particle Viscosity. *Chem. Sci.* **2016**, *7* (2), 1298–1308. https://doi.org/10.1039/C5SC03223G.
(33) Price, H. C.; Mattsson, J.; Murray, B. J. Sucrose Diffusion in Aqueous Solution. *Phys. Chem. Chem. Phys.* **2016**, *18* (28), 19207–19216. https://doi.org/10.1039/C6CP03238A.
(34) Evoy, E.; Kamal, S.; Patey, G. N.; Martin, S. T.; Bertram, A. K. Unified Description of Diffusion Coefficients from Small to Large Molecules in Organic–Water Mixtures. *J. Phys. Chem. A* **2020**, *124* (11), 2301–2308. https://doi.org/10.1021/acs.jpca.9b11271.
(35) Evoy, E.; Maclean, A. M.; Rovelli, G.; Li, Y.; Tsimpidi, A. P.; Karydis, V. A.; Kamal, S.; Lelieveld, J.; Shiraiwa, M.; Reid, J. P.; Bertram, A. K. Predictions of Diffusion Rates of Organic Molecules in Secondary Organic Aerosols Using the Stokes-Einstein and Fractional Stokes-Einstein Relations. *Atmospheric Chemistry and Physics Discussions* **2019**, 1–24. https://doi.org/10.5194/acp-2019-191.
(36) Chang, P.; Gao, X.; Cai, C.; Ma, J.; Zhang, Y. Effect of Waiting Time on the Water Transport Kinetics of Magnesium Sulfate Aerosol at Gel-Forming Relative Humidity Using Optical Tweezers. *Spectrochimica Acta Part A: Molecular and Biomolecular Spectroscopy* **2020**, *228*, 117727. https://doi.org/10.1016/j.saa.2019.117727.
(37) Richards, D. S.; Trobaugh, K. L.; Hajek-Herrera, J.; Price, C. L.; Sheldon, C. S.; Davies, J. F.; Davis, R. D. Ion-Molecule Interactions Enable Unexpected Phase Transitions in Organic-Inorganic Aerosol. *Science Advances* **2020**, *6* (47), eabb5643. https://doi.org/10.1126/sciadv.abb5643.
(38) Davies, J. F. Mass, Charge, and Radius of Droplets in a Linear Quadrupole Electrodynamic Balance. *Aerosol Science and Technology* **2019**, *53* (3), 309–320. https://doi.org/10.1080/02786826.2018.1559921.

(39) Price, C. L.; Bain, A.; Wallace, B. J.; Preston, T. C.; Davies, J. F. Simultaneous Retrieval of the Size and Refractive Index of Suspended Droplets in a Linear Quadrupole Electrodynamic Balance. *J. Phys. Chem. A* **2020**, *124* (9), 1811–1820. https://doi.org/10.1021/acs.jpca.9b10748.
(40) Choczynski, J. M.; Kaur Kohli, R.; Sheldon, C. S.; Price, C. L.; Davies, J. F. A Dual-Droplet Approach for Measuring the Hygroscopicity of Aqueous Aerosol. *Atmos. Meas. Tech.* **2021**, *14* (7), 5001–5013. https://doi.org/10.5194/amt-14-5001-2021.
(41) Preston, T. C.; Reid, J. P. Determining the Size and Refractive Index of Microspheres Using the Mode Assignments from Mie Resonances. *J. Opt. Soc. Am. A* **2015**, *32* (11), 2210. https://doi.org/10.1364/JOSAA.32.002210.
(42) Price, C. L.; Bain, A.; Wallace, B. J.; Preston, T. C.; Davies, J. F. Simultaneous Retrieval of the Size and Refractive Index of Suspended Droplets in a Linear Quadrupole Electrodynamic Balance. *J. Phys. Chem. A* **2020**, *124* (9), 1811–1820. https://doi.org/10.1021/acs.jpca.9b10748.
(43) Rickards, A. M. J.; Song, Y.-C.; Miles, R. E. H.; Preston, T. C.; Reid, J. P. Variabilities and Uncertainties in Characterising Water Transport Kinetics in Glassy and Ultraviscous Aerosol. *Phys. Chem. Chem. Phys.* **2015**, *17* (15), 10059–10073. https://doi.org/10.1039/C4CP05383D.
(44) Zuend, A.; Marcolli, C.; Luo, B. P.; Peter, T. A Thermodynamic Model of Mixed Organic-Inorganic Aerosols to Predict Activity Coefficients. *Atmospheric Chemistry and Physics* **2008**, *8* (16), 4559–4593. https://doi.org/10.5194/acp-8-4559-2008.
(45) Zuend, A.; Marcolli, C.; Booth, A. M.; Lienhard, D. M.; Soonsin, V.; Krieger, U. K.; Topping, D. O.; McFiggans, G.; Peter, T.; Seinfeld, J. H. New and Extended Parameterization of the Thermodynamic Model AIOMFAC: Calculation of Activity Coefficients for Organic-Inorganic Mixtures Containing Carboxyl, Hydroxyl, Carbonyl, Ether, Ester, Alkenyl, Alkyl, and Aromatic Functional Groups. *Atmos. Chem. Phys.* **2011**, *11* (17), 9155–9206. https://doi.org/10.5194/acp-11-9155-2011.
(46) Murata, T.; Lee, M.-S.; Tanioka, A. An Application of Percolation Theory to the Electrolyte Penetration through Porous Water-Swollen Cellulose Triacetate Membrane. *Journal of Colloid and Interface Science* **1999**, *220* (2), 250–254. https://doi.org/10.1006/jcis.1999.6529.
(47) Ellis, A. J. Partial Molal Volumes of MgCl2, CaCl2, SrCl2, and BaCl2 in Aqueous Solution to 200°. *J. Chem. Soc. A* **1967**, No. 0, 660–664. https://doi.org/10.1039/J19670000660.
(48) Tokita, M. Transport Phenomena in Gel. *Gels* **2016**, *2* (2), 17. https://doi.org/10.3390/gels2020017.